Vibrational distributions and rate constants from reactions of oxygen atoms with HI, GeH4, SiH4, H2Se, and H2S

B. S. Agrawalla and D. W. Setser

Citation: The Journal of Chemical Physics **86**, 5421 (1987); doi: 10.1063/1.452566
View online: http://dx.doi.org/10.1063/1.452566
View Table of Contents: http://scitation.aip.org/content/aip/journal/jcp/86/10?ver=pdfcov
Published by the AIP Publishing

Vibrational distributions and rate constants from reactions of oxygen atoms with HI, GeH_4, SiH_4, H_2Se, and H_2S

B. S. Agrawalla and D. W. Setser
Chemistry Department, Kansas State University, Manhattan, Kansas 66506

(Received 8 September 1986; accepted 29 January 1987)

The $OH(v \geqslant 0)$ distributions from the title reactions have been measured in a flowing-afterglow reactor using infrared chemiluminescence and laser-induced fluorescence techniques, which give the $OH(v \geqslant 1)$ and $OH(v \leqslant 1)$ distributions, respectively. The measured $OH(v = 0)$ relative population confirmed previous estimates for $OH(v = 0)$ populations based on extrapolations of linear surprisals using a three-body prior. The $\langle f_V(OH) \rangle$ values closely resemble the $\langle f_V(HF) \rangle$ and $\langle f_V(HCl) \rangle$ values from the corresponding F and Cl atom reactions, suggesting similar dynamics for H abstraction by $O(^3P)$, $F(^2P)$, and $Cl(^2P)$ atoms. The room temperature rate constants for OH formation are $4.2 \pm 0.5 \times 10^{-12}$ (GeH_4), $2.1 \pm 0.8 \times 10^{-12}$ (H_2Se), $1.2 \pm 0.4 \times 10^{-12}$ (SiH_4), and $\leqslant 3.8 \times 10^{-14}$($H_2S$)$cm^3$ $molecule^{-1}$ s^{-1}, which are 2–3 orders of magnitude lower than for the corresponding $F(^2P)$ and $Cl(^2P)$ atom reactions. Formation of OH is not the major product channel from $O + PH_3$; however, for certain conditions there are fast secondary reactions that can lead to strong OH chemiluminescence.

I. INTRODUCTION

The reactions of $O(^3P)$ with hydrogen containing molecules are important in combustion and oxidation processes and, although the macroscopic kinetics, especially for hydrocarbons, have been studied extensively, the microscopic aspects of the mechanisms are not well established. The initial step in reactions with saturated hydrocarbons and inorganic hydrides is usually abstraction of a hydrogen atom. The OH product is very reactive, and undergoes further reactions. Our present interest is the nascent OH vibrational distribution from hydrogen abstraction by $O(^3P)$ atoms and the dynamical interpretations that can be made from these distributions. The $OH(v,J)$ distribution can be studied at the state-to-state level by infrared chemiluminescence (IRCL) or laser-induced fluorescence (LIF). Due to predissociation of $OH(A)$,[1,2] the determination of vibrational populations for levels $v \geqslant 2$ is difficult by LIF.[3–5] Fortunately, the IRCL technique provides a way to observe $OH(v \geqslant 1)$ levels. In the present study IRCL and LIF measurements in a fast flow reactor (FR) were combined to obtain the complete nascent $OH(v)$ distributions for the HI, GeH_4, and H_2Se reactions and LIF alone was used to obtain the $OH(v = 0$ and $1)$ distribution for the less exoergic SiH_4 and H_2S reactions. The H_2S/H_2Se and SiH_4/GeH_4 pairs provide a representative view of H abstraction from group VI and IV hydrides, respectively. These OH vibrational distributions are compared to the HF and HCl distributions from hydrogen abstraction by $F(^2P)$ atom and $Cl(^2P)$ atom reactions and to the OH distributions from $O(^1D)$ atom reactions.

The $O(^3P) + HI$ and GeH_4 reactions previously were studied using IRCL from a flow reactor for 0.3 ms reaction time with 0.7 Torr Ar carrier gas[6] in order to demonstrate that IRCL from the fast flow reactor could give nascent OH vibrational distributions. The $OH(^2\Pi_{1/2,3/2})$ rotational and spin–orbit distributions were Boltzmann.[6] Although the observation time was somewhat shorter in the present study, the rotational and spin state distributions still were Boltzmann. Since the IRCL fast flow reactor method, including the problem of secondary reactions, has been extensively discussed,[7(a),7(c)] the experimental technique will not be emphasized in this paper. The secondary reactions can affect studies with $OH(v)$ in several ways. Secondary reactions between O atoms and the radical may provide an additional source of $OH(v)$, but that probably is less serious than for Cl or F atom reactions because of alternate exit channels for O atoms with radicals. Secondary reactions also may remove $OH(v)$ by the $OH(v) + O$ or $OH +$ reagent reactions. The kinetic criterion for a significant contribution from secondary removal reactions is basically the same as for secondary formation steps for the F or Cl atom reactions and the role of secondary reactions is discussed when the nascent $OH(v)$ distributions are presented in the Sec. IV.

The $OH(v = 0)$ populations previously[6] were estimated from extrapolation of linear surprisals, which were based on three prior models[8,9]—(i) a three-body model in which the polyatomic radical product is treated as an atom, (ii) expansion of the three-body model to include the rotational degrees of freedom of the polyatomic product, and (iii) a model including all internal and rotational degrees of freedom of the radical product. The LIF measurements of $OH(v = 0)$ populations permit a check of the best extrapolation (and by inference the best reference prior). In the present work we also measured the rate constants for $OH(v \geqslant 0)$ formation for the reactions of $O(^3P)$ with GeH_4, SiH_4, H_2Se, and H_2S relative to that for $O(^3P) + HI$ from measurement of the relative $[(OH, v \geqslant 0)]$ for a fixed [O] and reaction time from pairwise comparison of HI and the reagent of interest. The absolute rate constant for HI then gives the 300 K rate constant for the other molecules. Molecular beam studies[10,11] of $O(^3P) +$ hydrocarbon reactions provide OH rotational state distributions for H abstraction reaction of less exoergicity. By combining all the experimental results, a good over-

 0021-9606/87/105421-12$02.10

all view point can be obtained for the energy disposal and dynamics of H abstraction by $O(^3P)$ atoms.

II. EXPERIMENTAL TECHNIQUES

The 4 cm diam Pyrex flow reactor for IRCL and LIF experiments has been described.[7] The O atoms were produced by microwave discharge (60 W, 2450 MHz) in a flowing Ar/O_2 mixture. The 8 mm i.d. Pyrex discharge tube and flow line, which contained a right angle bend with a Wood's horn to reduce the scattered light, used to introduce the O atom flow to the reactor was coated with phosphoric acid to prevent O atom recombination. Hydrogen atoms, used to generate OH from the $H + NO_2$ reactions, were prepared by exchanging the H_2 for O_2 in the microwave discharge flow line just mentioned. Typically, 1–10 μmol s^{-1} of O_2 as a 20% mixture with Ar were combined with 700 μmol s^{-1} of Ar carrier gas; these flows were introduced separately at the front of the flow reactor. The [O] will be quoted on the assumption that 50% dissociation of O_2 was achieved. The Ar carrier gas was purified by passing the flow through a series of cooled molecular sieve filled traps. The reagents (HI, SiH_4, etc.) were stored as dilute mixture (1/10 to 1/50) in Pyrex glass reservoirs and introduced through a perforated glass ring located 1.5 cm upstream from the center of the NaCl observation window and 12 cm downstream of the O-atom inlet. The reaction time was 0.1 ms for the maximum pumping speed at 0.65 Torr pressure. The reagent gases HI, GeH_4, SiH_4, H_2S, PH_3, and NO_2 were obtained from Matheson; H_2Se was from Scientific Gas Products; H_2, O_2, and Ar were obtained from Airco. All reagents, except O_2 and H_2, were purified by freeze–pump–thaw cycles and vacuum distillation. All gas flows were metered, so that concentrations in the flow reactor are known; the typical concentrations were in the $1.0–25\times10^{12}$ molecule cm^{-3} range for the reagents, as well as the O atoms. In previous work with [F] or [Cl], lower concentrations were used because the reaction rates for Cl and F atoms are faster than for O atoms.

The IRCL measurements were made with a Digilab (FTS-20) Fourier transform spectrometer equipped with a liquid N_2-cooled InSb detector and a CaF_2/Fe_2O_3 beam splitter. Resolution of 1 or 2 cm^{-1} gave fully resolved OH rotational lines. The detector response was calibrated for the 2000–8000 cm^{-1} range with a 1000 C black body and a quartz–iodine reference lamp. In this study the rotationless Einstein coefficients of Meyer and Rosmus[6,12] and the line strength factors of Mies[13] were combined to obtain the Einstein coefficients for $OH(vJ)$ to convert the vibrational–rotational intensities to $OH(v)$ populations. Since the OH rotational distributions were strictly 300 K Boltzmann, the strongest emission lines were used to obtain the relative vibrational distributions. The LIF measurements were made using a flash lamp-pumped dye laser (Chromatix model CMX-4) equipped with doubling crystals; Rhodamine 6G and Fluorol 555 (Exciton Chemical Co.) dyes were used. Since our CMX-4 laser (1 μs pulse width, 6 cm^{-1} bandpass) did not scan in the ultraviolet, excitation spectra could not be recorded and the LIF was identified from the wavelength-resolved emission spectra using a 0.3 m McPherson monochromator with 300 nm blazed grating and a Hammamatsu R212UH PMT. The total $OH(A–X)$ fluorescence signals were obtained using narrow bandpass filters and another R212UH PMT. The $OH(A)$ lifetime is sufficiently long that rotational relaxation in the upper state is complete and fully developed bands are observed even though individual rotational levels were excited. A boxcar (PAR model 162/164) was used for integrating and averaging the emission signal. In all of this work, the LIF intensity was limited by the laser intensity, i.e., the transitions were not saturated.

Individual rotational lines of the $OH(A\leftarrow X)$ transition were excited in the LIF experiments and conversion of the LIF intensities to relative $v''=1$ and $v''=0$ vibrational populations were straightforward. For the $OH(v''=0)$ population measurement, the rotational lines of the $(1\leftarrow0)$ band were pumped and the $(1\rightarrow1)$ fluorescence was measured to determine $N_{0,J}$. For $OH(v''=1)$ the rotational lines of the $(1\leftarrow1)$ band were pumped and the $(1\rightarrow0)$ intensity was measured to determine $N_{1,J}$. The fluorescence intensity, $I_{v_0''J_0''}$, in photons s^{-1} for excitation of a $OH(v''=0,J'')$ level is given by

$$I_{v_0''J_0''}=\alpha N_{v_0''J_0''}B_{v_1'J_1'\leftarrow v_0''J_0''}P_{v_0''J_0''}A_{v_1'\rightarrow v_1''}T_{v_1'v_1''}, \tag{1}$$

where α is a constant, $n_{v_0''J_0''}$ is the concentration (molecule cm^{-3}) in the J_0'' level, $B_{v_1'J_1'\leftarrow v_0''J_0''}$ is the Einstein coefficient for stimulated absorption, $P_{v_0''J_0''}$ is the laser intensity in photons s^{-1} at $\nu_{v_1'J_1'\leftarrow v_0''J_0''}$, $A_{v_1'\rightarrow v_1''}$ is the Einstein coefficient for spontaneous emission (for the $1\rightarrow1$ band) and $T_{v_1'\rightarrow v_1''}$ is the transmission of the filter. The observed fluorescence $I^f_{v_0''J_0''}$ and laser power monitoring signal, $P^f_{v_0''J_0''}$, in erg s^{-1}, were divided by $\nu_{v_1'\rightarrow v_1''}$ and $\nu_{v_1'J_1'\leftarrow v_0''J_0''}$, respectively, and equated to $I_{v_0''J_0''}$ and $P_{v_0''J_0''}$. The OH Einstein coefficients are known[14,15] and need not be simplified to Franck–Condon factors. The subscripts $v_1'\rightarrow v_1''$ are used for fluorescence instead of $v_1'J_1'\leftarrow v_0''J_0''$, because the excited $OH(A,v'J')$ level relaxes to a 300 K rotational distribution without quenching[16] for our conditions. An equation similar to (1) can be written for the excitation of a rotational line in the $(1\leftarrow1)$ band (i.e., $v_1'J_1'\leftarrow v_1''J_1''$), and fluorescence observation from $(1\rightarrow0)$ band; taking the ratio of equations for $v'=0$ and 1 and rearranging terms gives the ratio of populations:

$$\frac{N_{v_1''J_1''}}{N_{v_0''J_0''}}=\frac{I^f_{v_1''}/P^f_{v_1''}}{I^f_{v_0''}/P^f_{v_0''}}\left(\frac{\nu_{v_1'\rightarrow v_1''}}{\nu_{v_1'\rightarrow v_0''}}\right)^2 \times\frac{(B_{v_1'J_1'\leftarrow v_0''J_0''})(A_{v_1'\rightarrow v_1''})(T_{v_1'\rightarrow v_1''})}{(B_{v_1'J_1'\leftarrow v_1''J_1''})(A_{v_1'\rightarrow v_0''})(T_{v_1'\rightarrow v_0''})}. \tag{2}$$

Here the $\nu_{v_1'J_1'\rightarrow v_1''J_1''}$ and $\nu_{v_1'J_1'\rightarrow v_0''J_0''}$ were set as the frequencies of the band centers, $\nu_{v_1'\rightarrow v_1''}$ and $\nu_{v_1'\rightarrow v_0''}$, respectively. Equation (2) is expressed for excitation from the same rotational level for both $v''=1$ and 0, so that Eq. (2) also gives the ratio of vibrational state population, $N_{v_1''}/N_{v_0''}$. If different rotational lines are used, then $N_{v_1''J_1''}$ and $N_{v_0''J_0''}$ must be divided by their respective 300 K Boltzmann fractions to give $N_{v_1''}/N_{v_0''}$. All the terms except the I and P terms in the right-hand side of

Eq. (2) are constants for a given set of conditions including laser frequency. For example, if the Q_1 branch $J = 3/2$ line is pumped, $\nu_{v_1' v_1''} = 31893\ \text{cm}^{-1}$, $\nu_{v_1' v_0''} = 35461\ \text{cm}^{-1}$, $B_{v_1' J_1' \leftarrow v_0'' J_0''}/B_{v_1' J_1' \leftarrow v_1'' J_1''} = 240/567$,[14] $A_{v_1' \rightarrow v_1''}/A_{v_1' \rightarrow v_0''} = 585/334$[14], and $T_{v_1' \rightarrow v_1''}/T_{v_1' v_0''} = 44/12$ (the transmission ratio of bandpass filters) and Eq. (2) reduces to Eq. (3):

$$\frac{N_{v_1''}}{N_{v_0''}} = \frac{N_{v_1'' J_1''}}{N_{v_0'' J_0''}} = \frac{I^f_{v_1'' J_1''}/P^f_{v_1'' J_1''}}{I^f_{v_0'' J_0''}/P^f_{v_0'' J_0''}} \times 2.21. \quad (3)$$

Excitation from several rotational levels were used to obtain reliable $\text{OH}(v'' = 1)/\text{OH}(v'' = 0)$ population ratios for a given reaction.

Since the fluorescence was observed from $\text{OH}(A, v' = 1)$ for pumping from both $v'' = 0$ and 1, any vibrational relaxation[16(d)] and electronic quenching[16(a)-16(c)] will affect the measurement of $N_{v_0''}$ and $N_{v_1''}$ in the same way. In fact, for our conditions of 0.5 Torr of Ar and $\leqslant 3\times10^{13}$ molecule cm^{-3} of reagent the vibrational relaxation and quenching is negligible relative to the radiative decay rate of $\text{OH}(A\ ^2\Sigma^+, v' = 1)$.[16]

III. RESULTS

A. LIF results for OH(X, v" =0,1)

The $H + NO_2$ reaction was studied for calibration purposes; high OH concentrations could be obtained for modest [H] and $[NO_2]$ so that the excitation wavelengths for selected OH rotational lines could be easily identified from the LIF spectrum. The P_1/P_0 ratio is well established[3-5] and the $H + NO_2$ reaction also was used to confirm the absence of OH vibrational relaxation for our experimental conditons. Figure 1 shows the $\text{OH}(A\text{-}X)$ fluorescence spectrum at 5 Å resolution from the $H + NO_2$ reaction. The $(1\rightarrow0)$ and $(1\rightarrow1)$ bands were obtained from excitation of the specified rotational lines of the $(1\leftarrow1)$ and $(1\leftarrow0)$ bands, respectively. The fluorescence, particularly the $\text{OH}(A,1\rightarrow X,1)$ band, appears as a poorly resolved double feature. The separation between the maximum of the $R_1 + R_{21}$ branch and the maximum of the five main branches plus the 140 cm^{-1} splitting between the $\text{OH}(^2\Pi_{1/2})$ and $\text{OH}(^2\Pi_{3/2})$ spin–orbit states is responsible for the shape of the fluorescence spectra at our resolution. Several J'' levels of $v'' = 1$ and 0 were pumped and the LIF intensities were consistent with a 300 K $\text{OH}(X,^2\Pi_{1/2,3/2})$ rotational Boltzmann distribution to within the 10% experimental uncertainty. These LIF experiments were done for 0.1 ms reaction time and for reaction conditions such that [OH] was first order in both $[NO_2]$ and [H] and the P_1/P_0 ratio, as deduced from the LIF intensities, was independent of $[NO_2]$ and $[H_2]$. The P_1/P_0 ratios obtained from several rotational lines are given in Table I and compared with results from molecular beam studies.[3-5] The average value, $P_1/P_0 = 0.69 \pm 0.13$, is in agreement with other work, which confirms (i) that our technique is reliable and (ii) that the OH vibrational relaxation was negligible. For the O atom abstraction reactions, the laser excitation wavelength was always selected by using the $H + NO_2$ system and then the reagent gas flows were switched to the O + HR reaction of interest.

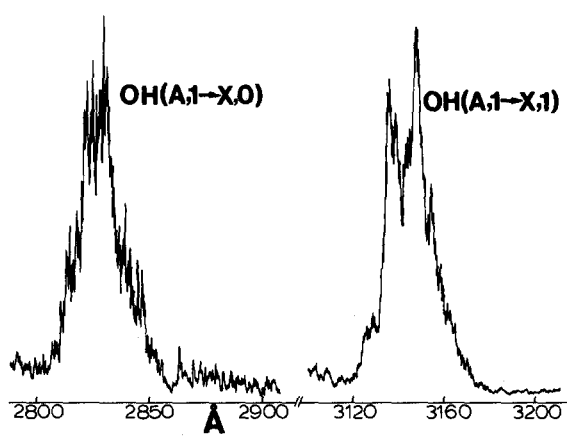

FIG. 1. Laser-induced $\text{OH}(A\ ^2\Sigma^+, v' = 1\rightarrow X^2\Pi, v'' = 0,1)$ fluorescence spectrum (5 Å resolution) from the $H + NO_2$ reaction. A reaction time of ~1.2 ms for $[H_2] \approx 5\times10^{13}$ and $[NO_2] \approx 1\times10^{13}$ molecule cm^{-3} was used to obtain a spectrum with the monochromator.

TABLE I. Comparison of $\text{OH}(v'' = 0$ and 1) population ratios from $H + NO_2$.

Reference	OH transitions	P_1/P_0	Average
This work[a,b]	$R_1 + R_{21}$ $(K' = 1)$	0.75 ± 0.12	0.69 ± 0.13
	$R_1 + R_{21}$ $(K' = 2)$	0.61 ± 0.10	
	$R_1 + R_{21}$ $(K' = 3)$	0.59 ± 0.18	
	$Q_1 + Q_{12}$ $(K' = 1)$	0.74 ± 0.16	
	$Q_1 + Q_{12}$ $(K' = 2)$	0.74 ± 0.07	
Mariella *et al.* (Ref. 4)	$(1\leftarrow1)$ vs $(0\leftarrow0)$		0.71 ± 0.15
Silver *et al.* (Ref. 3)	$(1\leftarrow1)$ vs $(0\leftarrow0)$		0.77 ± 0.18
Murphy *et al.* [Ref. 5(a)]	$(1\leftarrow1)$ vs $(0\leftarrow0)$		0.80 ± 0.08

[a] In our experiments the LIF was observed from $v' = 1$ following excitation from either $v'' = 1$ or $v'' = 0$.

[b] The $[NO_2]$ and $[H_2]$ concentrations were 0.8 and 3.0×10^{12} molecule cm^{-3}, respectively, for these experiments.

The $O + GeH_4$ rate constant, 4.2×10^{-12} cm^3 molecule^{-1} s^{-1}, is about 30 times smaller than for $H + NO_2$ and the rate constants for SiH_4, HI, H_2S, and H_2Se are even smaller than for GeH_4, *vide infra*. Therefore, the LIF intensities were recorded with only moderate S/N ratios, because it was desirable to keep the reagent concentrations low to prevent $\text{OH}(v)$ vibrational relaxation. The first order dependencies of the LIF intensities for both $\text{OH}(v'' = 0)$ and $\text{OH}(v'' = 1)$ on $[GeH_4]$, $[SiH_4]$, $[H_2S]$, and [HI] are shown in Figs. 2(a) and 2(b). The P_1/P_0 ratios obtained from excitation of several rotational transitions with 0.1 ms reaction time (with the exception of the H_2Se reaction) are given in Table II. The $[O_2]$ in each case was $1.0\text{–}1.5\times10^{13}$ molecule cm^{-3}; this $[O] + [O_2]$ mixture did not give $\text{OH}(v)$ relaxation as shown by monitoring the $\text{OH}(v)$ distributions over this range of $[O_2]$. There is a general 30% uncertainty in the average P_1/P_0 values as a consequence of the S/N ratio in the measurements.

The $O + H_2Se$ reaction was studied several months

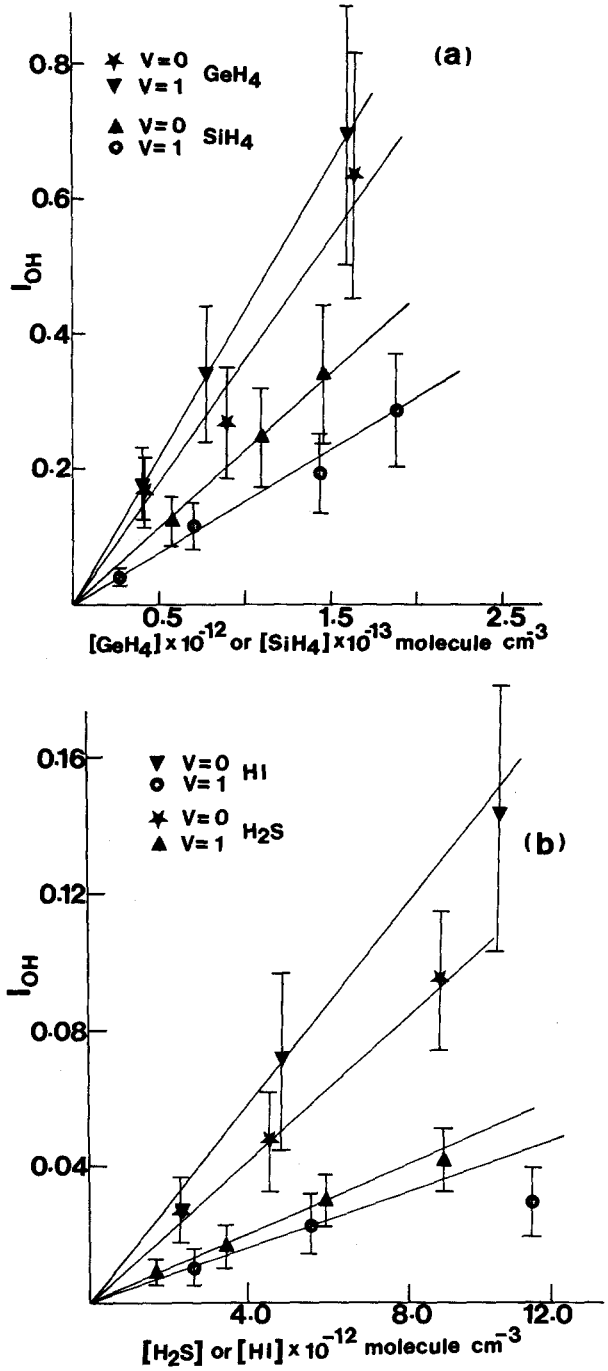

FIG. 2. Plots showing first order dependencies of the OH laser-induced fluorescence intensities from excitations of OH($v''=0$ and 1) from [GeH_4] and [SiH_4] in (a), and [H_2S] and [HI] in (b). The $Q_1+Q_{21}(J=3/2)$ line was excited in all cases except for GeH_4 for which $J=7/2$ was excited. The LIF intensities for O + SiH_4 have been reduced by a factor of 2 relative to O + GeH_4 for ease of presentation. The [O_2] was 1.0, 1.2, 1.5, and 1.5×10^{13} molecule cm^{-3} for GeH_4, SiH_4, H_2S, and HI, respectively, and Δt was 0.1 ms. The error bars display the $\pm$ 30% uncertainty associated with the signal-to-noise ratios of the LIF intensity measurements.

after the other reactions and the LIF signals were quite weak, presumably because the [O] was low. Therefore, the pumping speed was reduced in order to increase the [OH] and the reaction time became 0.3 ms rather than 0.1 ms. The longer time gave some relaxation because the P_1/P_0 ratio increased as [H_2Se] was reduced, and the nascent P_1/P_0 was estimated by extrapolation to zero [H_2Se].

We attempted to observe SH from the O + H_2S reaction, but the LIF signal from SH($A\leftarrow X$) excitation was not observable for 0.1 ms reaction time. A SH($v''=0$) signal was observed when the reaction time was increased to $\sim$1.5 ms; however, no attempt was made to measure the SH(v'') distribution since relaxation would have been extensive. Qualitative examination of O + D_2S for 1.5 ms reaction time showed LIF from both SD and OD. The O + SH reaction can yield SO($X,v''\leqslant15$). Although SO(A–X) LIF was not obervable for 0.1 ms reaction time, SO was easily detected[17] when the reaction time was increased to $\sim$1.5 ms.[17(b)] We plan to characterize the SO(X,v'') distribution in the future.

B. IRCL results from O atom reactions

The OH($v\geqslant1$) distributions from O + HI and GeH_4 were reported in an earlier IRCL study[6]; the O + H_2Se, H_2S, SiH_4, and PH_3 reactions were studied in this work and new measurements were done for HI to establish reference to the earlier work. An OH($\Delta v=1$) emission spectrum from O + H_2Se obtained at 0.7 Torr is shown in Fig. 3. No high J lines ($J\geqslant15/2$) were observed from either the OH($1\rightarrow0$) or ($2\rightarrow1$) transitions and the populations were strictly 300 K Boltzmann. The spectra from O + H_2Se were also recorded at 0.26 and 0.13 Torr, but emission from OH($J\geqslant15/2$) still was not observed. The OH($^2\Pi_{3/2}/^2\Pi_{1/2}$) population ratio was 2.0 $\pm$ 0.2 and independent of pressure. Thus, the rotational and the OH($^2\Pi_{3/2}$) and OH($^2\Pi_{1/2}$) distributions are 300 K Boltzmann under our experimental conditions. These conclusions match the findings from the previous study of the O + HI and GeH_4 reactions.[6]

The OH(v) intensities from the O + HI experiments were weaker than in our earlier work, even when the reaction time was increased to $\sim$0.3 ms. The reaction time in the earlier work was also 0.3 ms (the 0.45 ms time given in Ref. 6 should have been 0.3 ms since the pumping speed in the 5 cm diam flow reactor was 120 m s^{-1} according to our present flow calibration). The most likely explanations for the weaker OH(v) signals in this work is lower [O], as a consequence of reduced dissociation of O_2, or a deterioration of our InSb detector. The present discharge tube had a Wood's horn arrangement with a longer flow time from the discharge to the reaction zone and oxygen atom recombination may have been more extensive. The OH(v) distribution shown in Fig. 4(a) for HI showed a very small dependence on [HI] and extrapolation gave $P_1{:}P_2{:}P_3=0.13{:}0.39{:}0.48$, which is fortuitously identical to our earlier study (0.13:0.39:0.48 after adjustment to the Einstein coefficients of Meyer and Rosmus). The slight vibrational relaxation in Fig. 4(a) was not apparent in the earlier study and we have no good explanation for this difference.

Since the rate constant ($1.6\pm0.1\times10^{-12}$ cm^3 $molecule^{-1}$ s^{-1}) for O + HI is known,[18] this reaction was compared pairwise with H_2Se, SiH_4, and H_2S for the same [O] and reaction time in order to assign rate constants for OH($v\geqslant1$) formation. These experiments consist of measuring and plotting the [OH($v\geqslant1$)] concentration vs [HI] and [RH] under first order conditions[7] for the same [O]. The

TABLE II. OH($v''=0$ and 1) Ratios from the GeH_4, SiH_4, HI, H_2S, and H_2Se reactions.

Reaction[a]	OH transition[b]	Signal-to-noise ratio[c] OH($v''=1$)	Signal-to-noise ratio[c] OH($v''=0$)	P_1/P_0	Average
	R_1+R_{21} ($K'=1$)	7.0	2.0	1.49	
	R_1+R_{21} ($K'=2$)	7.0	2.0	1.38	
	R_1+R_{21} ($K'=3$)	7.0	1.8	2.04	
	Q_1+Q_{12} ($K'=1$)	8.0	1.7	2.20	
$O+GeH_4$	Q_1+Q_{12} ($K'=2$)	7.5	2.0	2.10	1.7 ± 0.3
	Q_1+Q_{12} ($K'=3$)	9.0	1.8	1.63	
	R_1+R_{21} ($K'=1$)	4.0	2.5	1.47	
	R_1+R_{21} ($K'=2$)	5.5	2.5	1.37	
	R_1+R_{21} ($K'=3$)	4.5	2.5	1.51	
	R_1+R_{21} ($K'=1$)	5.5	1.0	3.67	
$O+SiH_4$	R_1+R_{21} ($K'=2$)	6.0	1.0	4.46	4.2 ± 0.6
	Q_1+Q_{12} ($K'=1$)	6.0	1.5	4.03	
	Q_1+Q_{12} ($K'=2$)	6.5	1.5	4.82	
	R_1+R_{21} ($K'=1$)	0.7	0.7	0.64	
$O+HI$	R_1+R_{21} ($K'=2$)	0.7	0.7	0.75	0.8 ± 0.3
	Q_1+Q_{12} ($K'=1$)	1.1	1.3	0.70	
	Q_1+Q_{12} ($K'=2$)	1.1	0.8	1.08	
	Q_1+Q_{12} ($K'=1$)	1.8	0.8	1.60	
$O+H_2S$	Q_1+Q_{12} ($K'=2$)	1.9	0.9	1.13	1.2 ± 0.4
	Q_1+Q_{12} ($K'=3$)	2.0	0.7	0.85	
	Q_1+Q_{12} ($K'=1$)	5.0	2.5	1.55[d]	
$O+H_2Se$	Q_1+Q_{12} ($K'=2$)	6.0	3.0	1.62[d]	1.5 ± 0.2
	Q_1+Q_{12} ($K'=3$)	8.0	3.7	1.38[d]	

[a] See Table III for thermochemical data.

[b] The excitation scheme was based on excitation of $v'=1$ for both $v''=0$ and 1; the signal-to-noise refers to the LIF intensity vs the background signal.

[c] These signal-to-noise ratios are the typical values for the middle range of reagent concentrations, see Fig. 2.

[d] The H_2Se experiments were done for 0.3 ms reaction time and the P_1/P_0 ratio depended on $[H_2Se]$. The nascent ratio given in the table was obtained from extrapolation to zero $[H_2Se]$. The reaction time was 0.1 ms for all other reactions.

ratio of the slopes of these linear plots is the ratio of the OH($v\geqslant1$) formation rate constants. Since the P_0/P_1 ratio is known from the LIF measurements, the rate constant for formation of OH($v\geqslant0$) can be assigned by scaling.

The $O+H_2Se$ reaction was studied with 0.3 ms reaction time for which OH(v) spectra with reasonable S/N ratios were obtained. The emission was from OH($v=1$ and 2) only and OH($v=3$) was not observed within the limitation of our S/N, see Fig. 3. According to our thermochemistry, *vide infra*, formation of OH(v–3) would be barely possible and its absence may indicate that $\langle E\rangle$ should be reduced by 1–2 kcal mol^{-1}. The dependence of the OH(v) distributions upon $[H_2Se]$ and $[O_2]$ for 0.3 ms reaction time is shown in Figs. 4(b) and 4(c). The OH(v) distribution was constant with changes in $[O_2]$ with $P_1{:}P_2=0.52{:}0.48$ for $[H_2Se]=1.3\times10^{13}$ molecule cm^{-3}. The OH (v) distribution showed some relaxation with increasing $[H_2Se]$ and extrapolation was used to obtain the nascent distribution of $P_1{:}P_2=0.48{:}0.52$. The [OH($v=1$ and 2)] exhibited first order dependence on both $[O_2]$ and $[H_2Se]$ over the concentration ranges shown in Fig. 4. In view of the OH(v) distribution obtained from the O + HI reaction, which was studied under the same conditions, the distribution for H_2Se should be reliable, within the $\pm$ 15% statistical uncertainty. Comparison of the OH(v) relative intensities from HI and H_2Se gave $k(OH,v\geqslant1)=1.8\pm0.7\times10^{-12}$ cm^3 $molecule^{-1}$ s^{-1}. Including LIF data for $v=0$ gives $k(OH)=2.1\pm0.8\times10^{-12}$ cm^3 $molecule^{-1}$ s^{-1} for H_2Se.

Emission was observed only from OH($v=1$) from $O+SiH_4$, as would be expected from the available energy. The IRCL intensity was compared to that from O + HI for 0.3 ms reaction time to assign an OH($v=1$) formation rate constant. From the $k(OH,v=1)$ and the LIF P_1/P_0 ratio of 4.2 ± 0.6, $k(OH)=1.2\pm0.4\times10^{-12}$ cm^3 $molecule^{-1}$ s^{-1} was obtained for SiH_4.

Useful IRCL emission could not be obtained, even for the 0.3 ms reaction time, from $O+H_2S$ and PH_3. Since $k(O+H_2S)$ is two orders of magnitude smaller[19] than $k(O+SiH_4$ or $H_2Se)$ the low IRCL intensity is expected. Fortunately, the LIF signal from $O+H_2S$ was measurable, albeit with poor S/N ratios, and an estimate for the rate constant for OH($v=0$ and 1) formation could be obtained. The LIF intensities were compared for $O+H_2S$ and $O+GeH_4$, the *upper limit* to the OH formation rate constant from H_2S was set as 3.8×10^{-14} cm^3 $molecule^{-1}$ s^{-1} based on the GeH_4 rate constant mentioned above. This is in modest agreement with the $k(O+H_2S)$ value of 1.8×10^{-14} cm^3 $molecules^{-1}$ s^{-1}. The question of the displacement vs abstraction reaction channels for $O+H_2S$ is considered in Sec. IV.

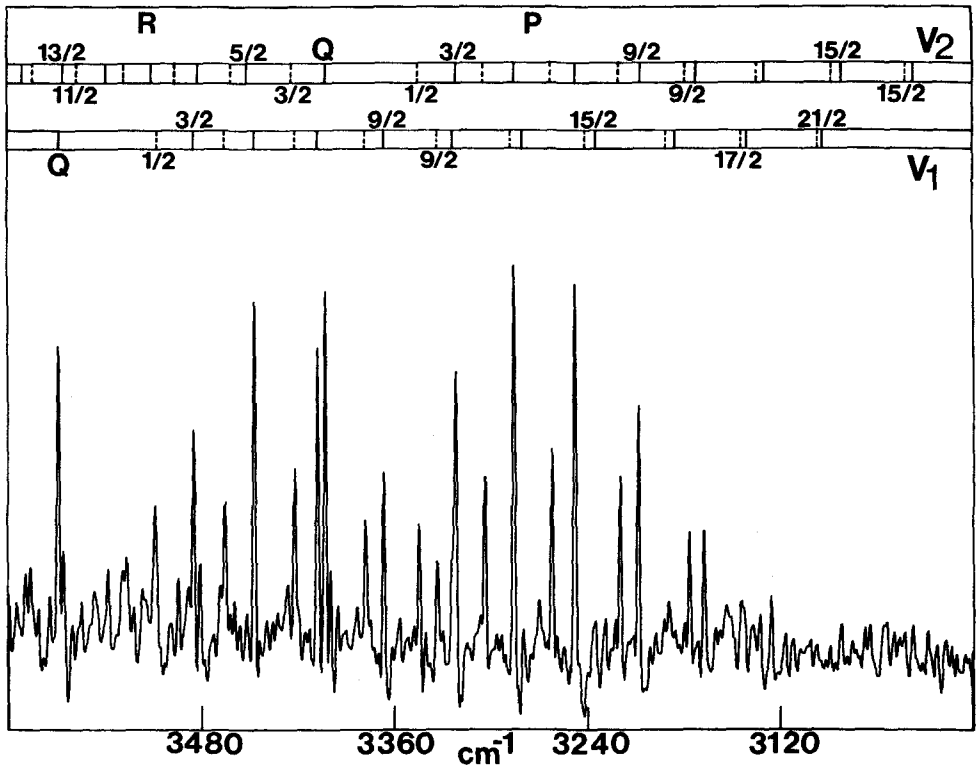

FIG. 3. The OH($\Delta v = 1$) infrared emission spectrum from $O + H_2Se$ at 2 cm^{-1} resolution. The $^2\Pi_{3/2}$ and $^2\Pi_{1/2}$ spin doublets are clearly resolved for the R and P branches; the upper labels are for the $^2\Pi_{3/2}$ state (solid lines) and the lower labels are for the $^2\Pi_{1/2}$ state (dotted lines). The Q branch lines are not resolved. The spectrum was recorded at 0.65 Torr, $\Delta t = 0.3$ ms, with $[O_2]$ and $[H_2Se] = 2.3\times10^{13}$ and 1.3×10^{13} molecule cm^{-3}, respectively. The number of interferometer scans for this spectrum was 128.

The $O + PH_3$ reaction is a complicated system.[20,21] The IRCL from OH could not be observed at the beginning of an $O + PH_3$ experiment. However, *very* strong OH (v) emission developed, even for 0.3 ms reaction time, after the reagents had flowed for a period of time. A rough comparison of the OH(v) relative intensity, after OH emission became observable, suggested that some reaction was giving OH(v) with a rate comparable to that for $O + HI$. When the OH emission was observable, the PH_3 inlet ring near the observation window always appeared to have a deposit of red phosphorus. Once this deposit was formed, there seemed to be a catalytic effect leading to OH(v) formation. The OH(v) spectrum from the O/PH_3 system included emission up to OH($v = 5$), whereas direct formation of OH from $O + PH_3$ can only give OH($v \leqslant 3$). The average OH(v) distribution for a range of $[O_2]$ and $[PH_3]$ was P_1–P_5 = 0.24:0.28:0.23:0.18:0.06. The OH($v \leqslant 5$) emission from the O/PH_3 system is mysterious because it is so strong. Stedman and co-workers[20(a)] have reported similar behavior for the visible chemiluminescence in the $O + PH_3$ system, i.e., the intensity is greatly enhanced whenever the red phosphorous deposit is present. Strong visible emission extending from the PH_3 inlet to the end of the flow reactor with the intensity increasing with distance was also observed in our experiments. Scanning the emission with a monochromator showed a band system at 320–330 nm and a strong continuum between 360–800 nm. These emissions are discussed by Stedman and co-workers. Based upon early literature,[20(b)] $O + PH_3$ has been considered to be a slow reaction. However, Hamilton and Murrels[21] demonstrated that the O atom removal rate constant is 4.6×10^{-11} cm^3 molecule^{-1} s^{-1}, and that the products are $H_2PO + H$. The lack of observable IRCL from the primary step is because of the domination by the displacement channel. Further work is necessary to understand the reactions that give vibrationally excited OH.

C. Thermochemical considerations

The available energy from OH formation is defined by the standard relation with $n = 3$ and 5/2 for polyatomic and diatomic reagents, respectively;

$$\langle E \rangle = D_0(\text{OH}) - D_0(\text{H–R}) + E_a + nRT. \qquad (4)$$

The thermochemical data are summarized in Table III. The bond energies for some of the reagents are not well known and were assigned from the thermochemical limits imposed by the HF(v,J) states observed from $F(^2P) + RH$ reactions together with consideration of the literature. The activation energies, E_a, for the $O + HR$ reactions are generally not available and we based the entries in Table III on the E_a for the $F + HR$ reactions and the ratios of rate constants of $O(^3P)$ atom reactions; these calculations are given in the footnotes of Table III. In making the calculation we assumed that the F and O atom reactions had the same preexponential factors. The rate constants and activation energies for the F atom reactions were taken from Ref. 7, except for PH_3 which was reported in Ref. 27. Although the exact E_a values for the F atom reactions are not well known, they are so small that the uncertainties are not important. As will become evident, there are two critical cases, GeH_4 and H_2Se, because the available energy is very close to the threshold for formation of OH($v = 3$), which requires 29.2 kcal mol^{-1}. Emission from OH($v = 3$) was observed from GeH_4 but not from H_2Se.

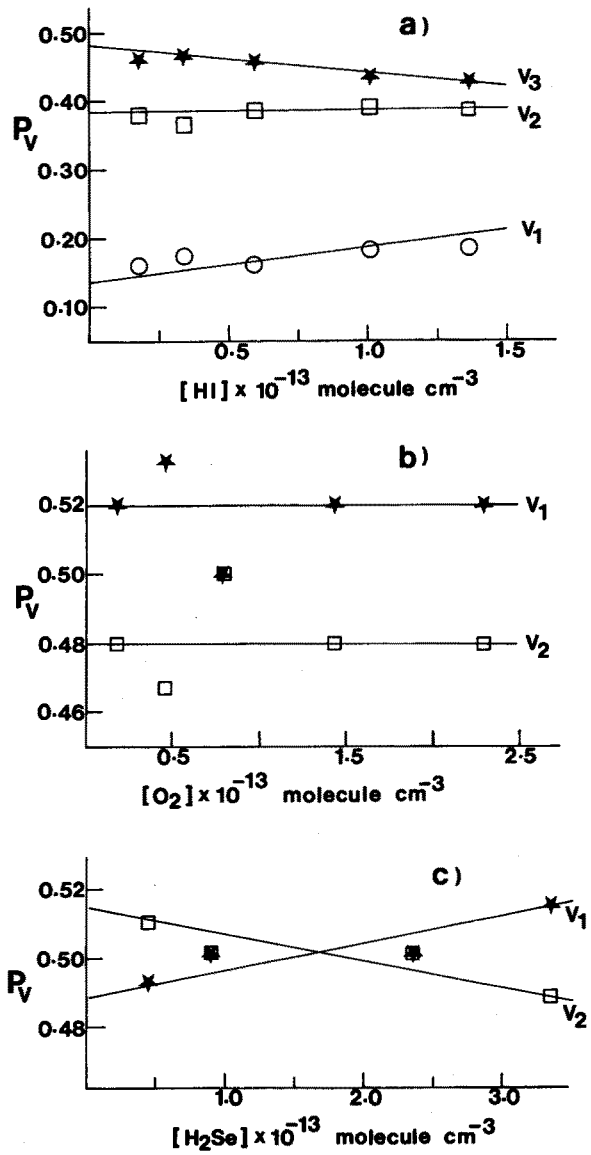

FIG. 4. The OH(v) distributions derived from IRCL for (a) O + HI plotted vs [HI], and (b) and (c) O + H_2Se plotted vs [O_2] and [H_2Se], respectively, at 0.65 Torr and $\Delta t = 0.3$ ms. The [O_2] was 7.9×10^{12} molecule cm^{-3} in (a) and (c) and [H_2Se] was 1.3×10^{13} molecule cm^{-3} in (b). The change in the distributions in plots (a) and (c) is attributed to relaxation by HI or H_2Se and the nascent OH(v) distributions were estimated by extrapolation to zero concentration. Explanation for the slightly different distributions for the [O_2] and [H_2Se] plots is given in the text.

TABLE III. Thermochemical data[a,b] (kcal mol^{-1}) for O(^3P) + RH reactions.

RH	D_0(ref)	$-\Delta H^\circ_0$	E_a[c]	$\langle E\rangle$[a,b]
HI	70.4 ± 0.1(22)	30.9 ± 0.5	3.0 ± 1.0[d]	35.4 ± 1.0
GeH_4	78.0 ± 1.0 (see the text)	23.3 ± 1.0	3.3 ± 1.0[e]	28.4 ± 2.0
SiH_4	90.0 ± 2.0 [24(b)]	11.3 ± 2.0	3.9 ± 1.0[f]	17.0 ± 2.5
H_2Se	76.0 ± 2.0 [25, 7(c)]	25.3 ± 2.0	3.1 ± 1.0[g]	30.2 ± 2.5
H_2S	90.5 ± 1.0 [26, 7(c)]	10.8 ± 1.0	6.2 ± 1.0[h]	18.8 ± 2.0
PH_3	79.0 ± 1.0 (26, 27)	22.3 ± 0.5	$\geqslant6.2\pm1.0$[i]	30.3 ± 2.0

[a] D°_0(O–H) was taken as 101.3 ± 0.5 kcal mol^{-1} (Ref. 22).
[b] The required energies for formation of $v=1$, 2, and 3 of OH($^2\Pi_{3/2}$) are 10.2, 19.9, and 29.2 kcal mol^{-1}, respectively.
[c] E_a was calculated from the ratio of the O + RH and corresponding F + RH rate constants assuming that the preexponential factors were the same; $E_a(\mathrm{O}+\mathrm{RH}) = E_a(\mathrm{F}+\mathrm{RH}) + RT\ln[k(\mathrm{F}+\mathrm{RH})/k(\mathrm{O}+\mathrm{RH})]$.
[d] In Ref. 7 $E_a = 2.0$ kcal mol^{-1} was used, but 3.0 kcal mol^{-1} is more consistent with the comparison for F + HI; $E_a(\mathrm{O}+\mathrm{HI}) = 1.0 + RT\ln(45/1.6) = 3.0$ kcal mol^{-1}; see Ref. 18..
[e] $E_a(\mathrm{O}+\mathrm{GeH_4}) = 0.5 + RT\ln(430/4.2) \sim 3.3$ kcal mol^{-1}.
[f] $E_a(\mathrm{O}+\mathrm{SiH_4}) = 0.5 + RT\ln(380/1.2) \sim 3.9$ kcal mol^{-1}.
[g] $E_a(\mathrm{O}+\mathrm{H_2Se}) = 0.5 + RT\ln(180/2.1) \sim 3.2$ kcal mol^{-1}.
[h] $E_a(\mathrm{O}+\mathrm{H_2S}) = 0.7 + RT\ln(160/0.018) \sim 6.2$ kcal mol^{-1}; if our upper limit value (4.8×10^{-14} cm^3 $molecule^{-1}$ s^{-1}) is used $E_a \sim 4.6$ kcal mol^{-1}.
[i] Since OH was not observed from the primary reaction, the E_a was taken to be larger than for H_2S.

The $D_0(H_3Ge–H)$ was based upon our recent F + GeH_4 study[7(c)] for which the highest observed state was HF($v=4,J=18$), which corresponds to 59.0 kcal mol^{-1}. Including $3RT$ (= 1.8 kcal mol^{-1}) thermal energy and $E_a = 0.5$ kcal mol^{-1} gives $D_0(H_3Ge–H) \leqslant 78.6$ kcal mol^{-1}. This is in agreement with the bond energy derived from the highest energy HF(v,J) states observed in an earlier arrested relaxation study.[23(a)] On the other hand, based on the thermochemistry of the $GeH_4 + I_2$ reaction, $D_0(H_3Ge–H) = 82.7\pm0.2$ kcal mol^{-1} has been recommended.[23(b)] However, the IRCL results are very reproducible for both FR and AR techniques and the highest observed HF(v,J) levels should provide a reliable upper limit to $D_0(H_3Ge–H)$; the best average value from the high J limit of several v levels is 78.0 ± 1.0 kcal mol^{-1}. In our previous report[6] of O + GeH_4, we used $D_0(H_3Ge–H) = 75.1$ kcal mol^{-1} and $E_a = 2.5$ kcal mol^{-1} to obtain $\langle E\rangle = 30.5$ kcal mol^{-1}; however, we now favor the somewhat lower value in Table III.

The thermochemistry for SiH_4[24] is well established and comparing the O and F atom rate constants suggest $E_a = 3.9$ kcal mol^{-1} with $\langle E\rangle = 17$ kcal mol^{-1}. This limit agrees with the lack of formation for OH($v=2$). The highest observed HF(v,J) levels from F + H_2S and H_2Se can be used to corroborate presently accepted bond energies.[25,26] The highest observed states from H_2S were HF($v=2,J=21$; $v=3,J=16$; $v=4,J=10$), which correspond to an energy of 47.0 ± 1.0 kcal mol^{-1} and D_0(H–SH) $= 90.5\pm1.0$ in good agreement with 91.1 ± 1.0 kcal mol^{-1} favored by McMillen *et al.*[26(b)] For F + H_2Se the highest observed states were HF($v=4,J=10$ and $v=5,J=12$) which, give D_0(H–SeH) $= 77\pm2$ kcal mol^{-1} in agreement with the 76 kcal mol^{-1} value of Dixon *et al.*[25] The ΔH°_0 values were combined with the room temperature rate constants to estimate E_a and $\langle E\rangle$. The E_a for abstraction from PH_3 was estimated by analogy to the O + H_2S reaction. For H_2Se the resulting $\langle E\rangle$ predicts that OH($v=3$) could have been formed; which is contrary to the experimental result. The recommended[28(a)] E_a for O atom removal by H_2S is 4.3 ± 0.4 kcal mol^{-1} and $E_a = 1.6\pm0.3$ kcal mol^{-1} has been reported[28(b)] for SiH_4 based upon rate constants for a 297–438 K range of temperature. It seems evident that the smaller rate constants for O atom reactions, relative to F atom reactions, are mainly because of larger E_a values, however, the procedure used to

estimate the values in Table III may give upper limits to the true E_a values.

IV. DISCUSSION

A. OH(v) formation rate constants and competing reaction channels

The OH formation rate constant is largest for GeH_4; the HI, SiH_4, and H_2Se rate constants are 2–3 times smaller and that for H_2S is 100 times smaller,[19(b)] than for H_2Se. The $O(^3P)$ rate constants are about two orders of magnitude smaller than the corresponding values for the $F(^2P)$ and $Cl(^2P)$ reactions,[11] even though the thermochemistry for the Cl and O atom reactions is similar. Comparison of the measured constants for Cl and O atom reactions with HBr confirm that the latter has the larger activation energy.[28–30] The most recent study[30(a)] of Cl + HBr reported a temperature independent rate constant of 3.4×10^{-12} cm^3 $molecule^{-1}$ s^{-1}; a prior study[30(b)] reported a rate constant that was 3 times smaller with an activation energy of -0.9 kcal mol^{-1}. The three most recent O + HBr studies have reported $4.0\times10^{-12}\exp-(2700/RT)$[29(a)]; $6.7\times10^{-12}\exp-(3100/RT)$,[29(b)] and $1.3\times10^{-11}\times\exp-(3610/RT)$[18] cm^3 $molecule^{-1}$ s^{-1}. The higher activation barriers, relative to $F(^2P)$ and $Cl(^2P)$ atom reactions, do not alter the dynamics of H abstraction by $O(^3P)$ atoms in a major way, as will be discussed in the next section. Our rate constant for SiH_4 can be compared to a measurement based upon O atom removal in a flash photolysis system.[28(b)] Their result, $0.5\pm0.1\times10^{-12}$ cm^3 $molecule^{-1}$ s^{-1}, is one-half as large as ours. Given the combined uncertainty from our intensity comparisons for SiH_4 and HI pair and the uncertainty in the absolute rate constant for HI,[18] the agreement is satisfactory. To our knowledge there are no other rate constant measurements that can be used for comparison.

A second difference, relative to F and Cl atom reactions, is the possible greater propensity for addition rather than abstraction for oxygen atoms with second and third row hydrides. The $O(^3P) + H_2S$ reaction has received considerable attention and both abstraction and addition–displacement channels have been observed[19,31,32]:

$$O + H_2S \rightarrow OH + SH$$
$$\rightarrow HSO + H. \quad (5)$$

Our upper limit to the OH(v) formation rate constant ($\leqslant3.8\times10^{-14}$ cm^3 $molecule^{-1}$ s^{-1}), which is based upon the LIF measurements since IRCl was not observable, is not so different from the O atom removal rate constant (1.8×10^{-14} cm^3 $molecule^{-1}$ s^{-1}).[19(a)] Since OH($v=0$ and 1) was observed by LIF, we suspect that OH formation is the major channel at 300 K. From end product analysis in a photolytic system, Singleton and co-workers concluded[19(b)] that OH formation is the main channel. Clemo *et al.*[31] observed the HSO product in a molecular beam experiment, but they did not establish the branching fraction for HSO formation. Since HSO can be monitored by LIF,[33] a LIF study of $O + H_2S$ with simultaneous detection of OH, SH, and HSO is possible and with proper calibration such measurements could further characterize the branching fractions. The formation of SO(v'') at longer reaction times in the $O + H_2S$ system can be rationalized via O atom reaction with either HSO or HS and mere observation of SO does not add any information about the branching. Although not yet identified, the $O + H_2Se$ reaction may have an addition–displacement channel; the $O + PH_3$ reaction proceeds entirely by the displacement channel at 300 K.

B. Nascent OH(v) distributions from H abstraction

Although the O + HR reaction rates are slower than the analogous F and Cl atom reactions, the secondary reactions in the O atom systems probably are rapid. If the O + R reaction contributes a secondary source of OH(v), the ratio of the yields of the secondary to primary reactions[7] depends upon $k_{sec}[O]\Delta t/2$, rather than k_{pri}, and the yield ratio should be less than 0.10 for most of the operating conditions. Furthermore, the secondary reactions between O atoms and the radicals produced in the primary abstraction reactions probably do not give OH. Thus, contributions to the OH(v) yield from secondary reactions probably are less serious for O atom than is formation of HF(v) from secondary reactions with F atoms. For the O/HR/OH(v) system there also can be O + OH(v) and HR + OH(v) secondary reactions (with rate constants k'_{sec} and k''_{sec}) that remove OH(v). For short reaction times the ratio of the secondary removal steps to the primary formation step has the form, $(k'_{sec}[O] + k''_{sec}[HR])\Delta t/2$. For concentration of $[O] = [HR] = 10^{13}$ molecule cm^{-3}, $\Delta t = 0.1$ ms and $k'_{sec} = k''_{sec} = 5\times10^{-11}$ cm^3 $molecule^{-1}$ s^{-1} the ratio will be 0.05. Clearly longer times, higher reagent concentrations or larger rate constants make the situation worse. Empirical evidence that the secondary reaction effects are not serious come from two types of experiments.[7(a)] First, the [OH(v)] yields were first order in both [O] and [HR]. Second, the OH(v) vibrational distributions are insensitive to [O], as shown in Fig. 4(b) and similar unpublished plots. Figures 4(a) and 4(c) shows that the distributions are slightly dependent on [HR] in the 10^{13} molecule cm^{-3} regime. Since the vibrational relaxation rate constants may be larger than k'_{sec} or k''_{sec}, these data suggest that secondary removal reactions should not be important. Extrapolation to low reagent concentrations were done to eliminate the minor degree of relaxation observed in the IRCL data. Thus, the relative OH(v) product measurements from this work, which are summarized in Table IV, can be taken as good estimates of the *nascent* OH vibrational distributions.

The combined LIF and IRCL results give complete OH($v\geqslant0$) distributions. The P_0 values based upon linear extrapolation of surprisal plots with model I for HI and model I and II priors for H_2Se and GeH_4 are listed for comparison. The P_0 value from the GeH_4 distribution, P_0–$P_3 = 0.18{:}0.31{:}0.47{:}0.03$, is in good agreement with the $P_0 = 0.20$ value from extrapolation of a linear surprisal based on a three-body prior. For H_2Se the measured P_0 value is 0.24 ± 0.04, which also agrees better with the linear surprisal based on three-body prior than on a prior that includes the rotational degrees of freedom of the radical product. Since only OH($v\leqslant1$) is formed from $O + SiH_4$, the LIF experiments gave the complete OH(v) distributions,

TABLE IV. Summary of energy disposal and rate constants for O atom reactions.

Reaction $\langle E \rangle$ (kcal mol^{-1})	OH(P_1/P_0) LIF	OH distributions P_0	P_1	P_2	P_3	$\langle f_V \rangle$	Rate constant[a] (cm^3 molecule^{-1} s^{-1})	Reference
O + HI	0.8 ± 0.3		13	39	48			This work
(35.4)		13	11	34	42	0.56	1.6×10^{-12}	a
		02	13	38	47	0.64		
O + GeH_4	1.7 ± 0.5		38	57	04			This work
(28.4)		18	31	47	03	0.47	$4.3\pm0.5\times10^{-12}$	b
		20[c]	31	46	03	0.46		
		03[d]	37	55	04	0.56		
O + SiH_4	4.2 ± 0.6		100[e]					This work
(17.0)		19	81			0.49	$1.2\pm0.4\times10^{-12}$	This work
O + H_2S	1.2 ± 0.4	45	55			⩾0.30	$\leqslant3.8\times10^{-14}$	This work
(18.8)							1.8×10^{-14}	a
O + H_2Se	1.5 ± 0.2		48	52				This work
(30.3)		24	36	40		0.38	$2.1\pm0.8\times10^{-12}$	This work
		20[c]	38	42		0.40		
		13[d]	42	45		0.44		

[a] The O atom removal rate constants for HI and H_2S from Refs. 18 and 19(a), respectively. All other rate constant entries are for OH($v\geqslant0$) formation.
[b] The IRCL data including the rate constant measurement is from Ref. 6; the OH(v) distribution has been adjusted for use of the Einstein coefficients of Myer and Rosmus.
[c] P_0 based upon extrapolation of model I surprisal plot.
[d] P_0 based upon extrapolation of model II surprisal plot.
[e] Only OH($v=1$) was observed from IRCL.

P_0:P_1 = 0.19:0.81; the distribution is sharply peaked in $v=1$ and $\langle f_v(\mathrm{OH}) \rangle$ is 0.49, which is close to the result for GeH_4.

The P_0 and P_1 values for O + HI must be interpreted with some caution because the signal-to-noise ratio from the LIF measurements was poor for both $v=0$ and 1, since the populations were low. Within the limits of the uncertainty, $P_1 \simeq P_0$, which does not match the prediction from the linear surprisal extrapolation for *any* prior. For the O + HI reaction there is a possibility for two exit channels.

$$\mathrm{O + HI \rightarrow OH + I(^2P_{3/2})};\ \Delta H^\circ_0 = -30.9\ \text{kcal mol}^{-1}, \tag{6a}$$

$$\rightarrow \mathrm{OH + I(^2P_{1/2})};\ \Delta H^\circ_0 = -9.2\ \text{kcal mol}^{-1}. \tag{6b}$$

Even a minor contribution from the $I(^2P_{1/2})$ channel, which can give only OH($v\leqslant1$), could explain the unexpectedly high P_0 value. The $F(^2P)$ + HBr and HCl reactions yield ~10% of the $Br(^2P_{1/2})$ and $Cl(^2P_{1/2})$ channels, respectively[34–36]; however, F + HI gives negligible $I(^2P_{1/2})$ and the Cl + HBr and HI reactions do not give $Br(^2P_{1/2})$ or $I(^2P_{1/2})$.[35–38] We did not attempt to directly measure $I(^2P_{1/2})$ formation because of experimental problems,[39] and we are not aware of other work that explicitly checks for $I(^2P_{1/2})$ or $Br(^2P_{1/2})$ formation from O atom reactions with HBr or HI. The mechanism of $Br(^2P_{1/2})$ excitation in the F + HBr reaction is V–E transfer from vibrationally excited HF in the exit channel.[34,35] Such a process would require 3 quanta of vibrational energy or 2 quanta plus rotational energy of OH(v,J), but the open shell nature of OH could aid such a coupling to the I atom.

Formation of OH($v=2$, 19.9 kcal mol^{-1}) could be possible from O + H_2S, if the high E_a value selected here proves to be correct. The LIF experiments gave P_0:P_1 = 0.45:0.55, which corresponds to $\langle f_V \rangle \geqslant 0.3$. The value is quoted as a lower limit, since our $\langle E \rangle$ may be too high and the lack of IRCL data prevented detection of OH($v=2$). Although there is greater uncertainty for the H_2S results than for the other reactions, the apparent difference in energy disposal relative to SiH_4 is significant. The $\langle f_V(\mathrm{OH}) \rangle$ from H_2Se, which is based upon a more complete OH distribution, also is lower than for SiH_4 or GeH_4 and supports the trend just mentioned for H_2S. The $\langle f_V(\mathrm{HF}) \rangle$ from H_2S and H_2Se vs SiH_4 and GeH_4 also was lower for F atom reactions.[7]

The $\langle f_V(\mathrm{OH}) \rangle$ values in Table IV range from ~0.40 to 0.64, if H_2S is excluded because of the lack of IRCL data for OH($v=1$ and 2) and the uncertainty in $\langle E \rangle$. The energy disposal to HF by the corresponding F atom reactions show very similar trends for the different reagents, although the $\langle f_V(\mathrm{OH}) \rangle$ values are slightly smaller than $\langle f_V(\mathrm{HF}) \rangle$ for all cases, except HI. The $\langle f_V(\mathrm{HCl}) \rangle$ from Cl + HI, H_2S and H_2Se are also in broad agreement with the O atom reactions.[7,37] The Cl + GeH_4 reaction gave an anomalously low HCl(v) distribution with $\langle f_V(\mathrm{HCl}) \rangle = 0.24 \pm 0.03$ and a combination of abstraction and addition–elimination steps was suggested, although the experimental result probably should be checked.[37] The Cl + GeH_4 reaction does give some HCl($v=3$), which supports the $D_0(GeH_3 - H)$ value in Table III. The contrasting results for O + PH_3 (addition–displacement) vs Cl + PH_3 (normal abstraction) and

$O + GeH_4$ (normal abstraction) vs $Cl + GeH_4$ (anomalous abstraction or a combination of abstraction plus addition–elimination) provides evidence of how subtle differences in potential surfaces can alter the product channels for these reactions.

The steady-state OH rotational distributions were 300 K Boltzmann in the flow reactor and no information about rotational energy disposal was obtained except that levels above $N \sim 10$ probably are not formed. Several $O(^3P)$ + hydrocarbon reactions have been studied by the molecular beam-LIF technique and the OH rotational distributions, which were nearly identical for all hydrocarbons, decreased with increasing rotational energy.[10,11] There was no apparent preference for either λ-doublet component, but the $OH(^2\Pi_{3/2})$ state was favored over the $OH(^2\Pi_{1/2})$ state by a factor of 1.8. The lack of preference for specific λ-doublet states may be the absence of any obvious plane of symmetry for the abstraction reaction in collinear geometry (except for planar reagent molecules)[40] and/or because only low J levels are formed.[41] The absence of high rotational levels is fully consistent with the small reactive cross sections for oxygen atoms, which implies a collinear reaction pathway with small orbital angular momentum in the entrance channel. The various potential surfaces for $O(^3P)$ reaction with H_2 and other molecules give (for *ab initio* treatments) or assume (for semiempirical treatments) collinear transition states for abstraction.[40,42,43] Measurement of the rotational distributions for the more exoergic $O + GeH_4$, HI, and H_2Se reactions would be useful, but all indications are that only a small quantity of energy is released to OH rotational energy. This feature differs from the F and Cl atom reactions with *large* reactive cross sections for which the entrance channel orbital angular momentum can be converted to product angular momentum.[7,38]

C. Dynamics of $O(^3P)$ + RH abstraction reactions and comparison to $O(^1D)$

1. Reactions

The vibrational energy released to OH in hydrogen atom abstraction reactions is high and resembles the energy disposal to $HF(v)$ and $HCl(v)$ in F and Cl atom reactions. This similarity exist in spite of the fact that the $O(^3P)$ + RH reactions proceed over larger activation barriers. The kinematics associated with the H + L–H mass atom combination (H = heavy, L = light) overrides even major differences in potential surfaces for abstraction.[44] As a consequence of its light mass, the H atom jumps from the entrance channel to the exit channel resulting in a high degree of mixed energy release with efficient conversion of $\langle E \rangle$ to OH vibrational energy. On the other hand, the secondary interactions of the $OH(v,J)$ with the R group, which is another characteristic of the H + LH mass combination, may differ considerably from the reactions giving HF and HCl, because of the greater attraction between the $OH(v,J)$ and the open shell radical product. If the $OH(v,J)$ radical collides with R· before leaving the exit channel, it can recombine to give a chemically activated alcohol molecule, whereas the HF + R· secondary interactions are always less attractive and limited, at most, to H bonding interactions. Stated in another way, there is a crossing between the triplet abstraction potential surface and the ROH singlet surface. The secondary encounters may lead to a dynamically based potential surface coupling. More quantitative experimental studies with carefully selected reactants and quasiclassical trajectory studies on model surfaces are needed to quantify the effects of secondary encounters upon the energy disposal to $OH(v,J)$ vs $HF(v,J)$ for a common HR.

To further discuss possible difference between H atom abstraction by $O(^3P_{0,1,2})$ vs $F(^2P_{1/2,3/2})$ or $Cl(^2P_{1/2,3/2})$, it is useful to consider some potential surfaces in the literature. Dupuis and Lester[40] computed an *ab initio* abstraction surface for $O + H_2CO$. The H_2CO molecular plane defined the plane of symmetry in this system. They found a collinear transition state (for the oxygen–hydrogen–carbon atoms) and suggested that the $^3A'$ and $^3A''$ surfaces had similar properties, although the $^3A'$ was sketched as the lower surface. The $O + H_2CO$ surface was judged to be very similar to the $O(^3P) + H_2$ surface and further discussion will be given with respect to $O + H_2$, since a large amount of theoretical and experimental work has been done for both $O(^3P)$ and $O(^1D)$ reactions. The products $OH(^2\Pi) + H(^2S)$ correlate with $O(^3P) + H_2(^1\Sigma_g^+)$ via the lowest triplet state, $^3\Pi$, in collinear geometry.[42(c)] One significant difference, relative to F or Cl atom cases, is the $^3\Pi$ vs $^2\Sigma^+$ nature of the reactive surfaces with the possibility of Renner–Teller coupling for $O(^3P)$ atom surfaces.[45] Trajectory studies on several of the $O(^3P) + H_2$ potential surfaces appear to give reasonably good representations of the thermal rate constant[46]; however, the spin–orbit and λ-doublet effects have yet to be taken into account in these theoretical treatments.[46] The coupling of the reactive potential with the $O(^3P_{2,1,0}) + RH$ spin–orbit states is important since the Boltzmann $O(^3P_{2,1,0})$ population is 72:22:6. Andresen and Luntz[10] found that $OH(^2\Pi_{3/2})$ was favored over $OH(^2\Pi_{1/2})$ by a factor of 1.8 for $O(^3P)$ + hydrocarbon reactions and they suggested that this was a consequence of a correlation between the lowest energy $O(^3P_2)$ and the $OH(^2\Pi_{3/2})$ states.

There is considerable current interest in the $OH(v,J)$ nascent distributions from $O(^1D_2)$ atom reactions with simple polyatomic molecular hydrides.[47–50] The exoergicity is sufficiently large that several v levels can be produced and reaction with CH_4, larger hydrocarbons, NH_3 and H_2S have been investigated by LIF for $v = 0$ and 1 and by IRCL for $v \geqslant 1$. The $OH(v = 0$ and $1)$ rotational distributions seem to be two component in nature. The larger component includes the high rotational levels and can be characterized by a linear rotational surprisal; the much smaller component consists of low rotational levels. The former has generally been associated with insertion followed by prompt dissociation to $OH(v$, high $J)$ + R, and the latter is associated with direct abstraction by analogy with the low rotational distributions found for $O(^3P)$ atom reactions. The rotational distributions for $v \geqslant 2$ remain to be characterized. Recent chemiluminescence data[49] show that the $OH(v,J)$ distributions extend to high v levels, especially for $O(^1D) + CH_4$ and H_2S

and, in fact, the vibrational energy disposal resembles that found for $O(^3P_{2,1,0})$ atom reactions in this work. Given the accepted nature of the $O(^1D_2)$ reactions,[51] insertion probably is an important pathway and these higher $OH(v)$ levels must, at least in part, arise from collisions that begin as insertion reactions. The difficulty with this conclusion is that inverted OH vibrational distributions are not expected from dissociation of large chemically activated HOR* molecules. Luntz has suggested that abstraction by $O(^1D)$ can proceed in two ways. One way is by collinear approach with reaction taking place on a $^1\Pi$ surface correlating directly to OH. The second pathway involves the $^1A'$ surface (the insertion pathway) that correlates to ground state HOR; however, there will be a long range surface crossing between this $^1A'$ surface and the $^3A''$ component (of the $^3\Pi$ collinear potential) and, if the trajectory switches to the $^3A''$ surface, abstraction could result. In this context, our GeH_4, H_2Se, and HI data serve to characterize hydrogen abstraction by $O(^3P)$ atoms which gives inverted vibrational distributions with $\langle f_v(OH)\rangle = 0.45$–$0.55$. By implication, certain aspects of the $O(^1D)$ atom reactions seem to have abstraction-like dynamics.

V. CONCLUSION

Five $O(^3P)$ + RH exoergic reactions were studied in a fast flow reactor and nascent vibrational distributions and rate constants for $OH(v\geqslant 0)$ formation were obtained using a combination of laser-induced flourescence and infrared chemiluminescence techniques. The H abstraction rate constants for $O(^3P)$ reactions are 2–3 orders of magnitude smaller than for $F(^2P)$ or $Cl(^2P)$ reactions. The $\langle f_v(OH)\rangle$ values ranged from 0.4 to 0.6. The vibrational energy disposal to OH is similar to that for HF(HCl) for the corresponding F(Cl) reactions. The similarity is a consequence of the kinematics associated with the H–L–H mass combination, which overrides differences in potential energy for direct H-transfer reactions, and the larger activation barriers do not seriously alter the dynamics for O atom reactions relative to F(Cl) reactions. The laser-induced fluorescence measurements for $OH(v=0)$ confirm previous estimates of the $OH(v=0)$ populations deduced from extrapolation of linear surprisals based on the three-body model for the prior and infrared chemiluminescence data for $OH(v\geqslant 1)$. The $OH(v)$ distribution from these direct abstraction reactions may be useful for understanding the dynamics associated with "apparent" H atom abstraction by (O^1D) atom reactions.

ACKNOWLEDGMENTS

We thank Mr. S. Wategaonkar for assistance with some of the laboratory measurements and the reviewer for calling our attention to Ref. 28(b). This work was supported by the National Science Foundation (CHE-86-01599).

[1]K. R. German, J. Chem. Phys. **62**, 2584 (1975); **63**, 5252 (1975).
[2]G. H. Dieke and H. M. Crosswhite, J. Quant. Spectrosc. Radiat. Transfer **2**, 97 (1962).
[3]J. A. Silver, W. L. Dimpfl, J. H. Brophy, and J. L. Kinsey, J. Chem. Phys. **65**, 1811 (1976).
[4]R. P. Mariella, Jr., B. Lantzsch, V. T. Maxson, and A. C. Luntz, J. Chem. Phys. **69**, 5411 (1978).
[5](a) E. J. Murphy, J. H. Brophy, G. S. Arnold, W. L. Dimpfl, and J. L. Kinsey, J. Chem. Phys. **74**, 324 (1981); (b) E. J. Murphy, J. H. Brophy, and J. L.Kinsey, *ibid.* **74**, 331 (1981).
[6]B. S. Agrawalla, A. S. Manocha, and D. W. Setser, J. Phys. Chem. **85**, 2873 (1981); subsequent unpublished experiments for $H + NO_2$ gave $N(OH,v=1)/N(NO,v=1) = 2$–3 and $P_1{:}P_2{:}P_3 = 0.6{:}0.3{:}0.1$ for $NO(v)$. The $OH(v)$ relative populations reported in this work were deduced from the Einstein coefficients of Mies (Ref. 13).
[7](a) B. S. Agrawalla and D. W. Setser, in *Gas Phase Chemiluminescence and Chemi-ionization*, edited by A. Fontijn (North–Holland, Amsterdam, 1985). (b) B. S. Agrawalla and D. W. Setser, J. Phys. Chem. **88**, 657 (1984); (c) **90**, 2450 (1986).
[8](a) R. B. Bernstein and R. D. Levine, Adv. At. Mol. Phys. **11**, 215 (1975), (b) R. D. Levine and R. B. Bernstein, Acc. Chem. Res. **7**, 393 (1974).
[9]D. J. Bogan and D. W. Setser, J. Chem. Phys. **64**, 586 (1976).
[10](a) P. Andresen and A. C. Luntz, J. Chem. Phys. **72**, 5842 (1980); (b) A. C. Luntz and P. Andresen, *ibid.* **72**, 5851 (1980).
[11](a) K. Kleinermanns and A. C. Luntz, J. Chem. Phys. **77**, 3533, 3537, 3774 (1982); (b) H. J. Dutton, I. W. Fletcher, and J. C. Whitehead, J. Phys. Chem. **89**, 569 (1985).
[12]W. Meyer and P. Rosmus, J. Chem. Phys. **63**, 2356 (1975).
[13]F. H. Mies, J. Mol. Spectrosc. **53**, 150 (1974).
[14](a) D. R. Crosley and R. K. Lengel, J. Quant. Spectrosc. Radiat. Transfer **15**, 579 (1975); (b) I. L. Chidsey and D. R. Crosley, *ibid.* **23**, 187 (1980).
[15]W. L. Dimpfl and J. L. Kinsey, J. Quant. Spectrosc. Radiat. Transfer **21**, 233 (1979).
[16](a) K. Schofield, J. Phys. Chem. Ref. Data **8**, 223 (1979); (b) P. W. Fairchild, G. P. Smith, and D. R. Crosley, J. Chem. Phys. **79**, 1795 (1983); (c) R. A. Copeland and D. R. Crosley, *ibid.* **84**, 3099 (1986), and other papers in this series; (d) R. K. Lengel and D. R. Crosley, *ibid.* **68**, 5309 (1978).
[17](a) M. A. A. Clyne and I. S. McDermid, J. Chem. Soc. Faraday Trans. 2 **75**, 905 (1979); (b) B. S. Agrawalla, Ph.D. dissertation, Kansas State University, 1984.
[18]D. L. Singleton and R. J. Cvetanovic, Can. J. Chem. **56**, 2934 (1978).
[19](a) D. L. Singleton, R. S. Irwin, W. S. Nip, and R. J. Cvetanovic, J. Phys. Chem. **83**, 2195 (1979); (b) D. H. Singleton, G. Paraskevopoulos, and R. S. Irwin, *ibid.* **86**, 2605 (1982).
[20](a) M. E. Fraser, D. H. Stedman, and T. M. Dunn, J. Chem. Soc. Faraday Trans. 1 **80**, 285 (1984); (b) P. B. Davies and B. A. Thrush, Proc. R. Soc. London Ser. A **302**, 243 (1968).
[21]P. A. Hamilton and T. P. Murrells, J. Chem. Soc. Faraday Trans. 2 **81**, 1531 (1985).
[22]K. P. Huber and G. Herzberg *Molecular Spectra and Molecular Structure IV. Constants of Diatomic Molecules* (Van Nostrand, New York, 1979).
[23](a) K. C. Kim, D. W. Setser, and C. M. Bogan, J. Chem. Phys. **60**, 1837 (1974); (b) M. J. Almond, A. M. Doncaster, P. N. Noble, and R. Walsh, J. Am. Chem. Soc. **104**, 4718 (1982).
[24](a) W. H. Duewer and D. W. Setser, J. Chem. Phys. **58**, 2310 (1973); (b) A. M. Doncaster and R. Walsh, Int. J. Chem. Kinet. **13**, 503 (1981); (c) H. B. Schlegel, J. Phys. Chem. **88**, 6254 (1984).
[25]D. A. Dixon, D. Holtz, and J. L. Beauchamp, Inorg. Chem. **11**, 960 (1972).
[26](a) B. de B. Darwent, *Bond Dissociation Energies in Simple Molecules*, Natl. Bur. Stand. Data Ser. Natl. Bur. Stand. 31 (U.S. GPO, Washington, D.C., 1970); (b) D. F. McMillen and D. M. Golden, Annu. Rev. Phys. Chem. **33**, 493 (1982).
[27]A. S. Manocha, D. W. Setser, and M. A. Wickramaaratchi, Chem. Phys. **76**, 129 (1983).
[28](a) R. F. Hampson, Chemical Kinetic and Photochemical Data Sheets for Atmospheric Reactions, Report No. FAA-EE-80-17 to U.S. Dept. of Transportation (1980); (b) R. Atkinson and J. N. Pitts, Jr., Int. J. Chem. Kinet. **10**, 1151 (1978).
[29](a) R. D. H. Brown and I. W. M. Smith, Int. J. Chem. Kinet. **7**, 301 (1975); (b) D. F. Nava, S. R. Bosco, and L. J. Stief, J. Chem. Phys. **78**, 2443 (1983).
[30](a) J. L. Lamb, O. Kondo, and S. W. Benson, J. Phys. Chem. **90**, 941 (1986); (b) R. Rubin and A. Persky, J. Chem. Phys. **79**, 4310 (1983).
[31]A. R. Clemo, F. E. Davidson, G. L. Duncan, and R. Grice, Chem. Phys. Lett. **84**, 509 (1981).
[32]R. R. Smardzewski and M. C. Lin, J. Chem. Phys. **66**, 3197 (1977).

[33]M. Kawasaki, K. Kasatani, S. Tanahashi, H. Sato, and Y. Fujimura, J. Chem. Phys. **78**, 7146 (1983).
[34]J. P. Sung and D. W. Setser, Chem. Phys. Lett. **48**, 413 (1977).
[35]J. W. Hepburn, K. Liu, R. G. McDonald, F. J. Northrup, and J. C. Polanyi, J. Chem. Phys. **75**, 3353 (1981).
[36]M. A. A. Clyne and W. S. Nip, Int. J. Chem. Kinet. **10**, 367 (1978).
[37]M. A. Wickramaaratchi and D. W. Setser, J. Phys. Chem. **87**, 64 (1983).
[38]B. E. Holmes and D. W. Setser, in *Physical Chemistry of Fast Reactions Vol. 2 Reaction Dynamics*, edited by I. W. M. Smith (Plenum, New York, 1980).
[39]The rapid excitation–transfer reaction between $O_2(a^1\Delta)$ and $I(^2P_{3/2})$ makes the unambiguous assignment of $I(^2P_{1/2})$ formation from reaction (6b) very difficult, if the O atoms were prepared by a microwave discharge in O_2.
[40]M. Dupuis and W. A. Lester, Jr., J. Chem. Phys. **81**, 847 (1984).
[41]S. R. Leone, Annu. Rev. Phys. Chem. **35**, 109 (1984).
[42](a) R. Schinke and W. A. Lester, Jr., J. Chem. Phys. **70**, 4893 (1979); (b) S. P. Walch, T. Dunning, Jr., F. W. Bobrowicz, and R. Raffenetti, *ibid.* **72**, 406 (1980); (c) G. Durand and X. Chapuisat, Chem. Phys. **96**, 381 (1985); (d) J. N. Murrell and S. J. Carter, J. Phys. Chem. **88**, 4887 (1984).
[43]A. Persky and M. Broida, J. Chem. Phys. **81**, 4352 (1984).
[44](a) S. R. Leone, in *Gas-Phase Chemiluminescence and Chemi-Ionization*, edited by A. Fontijn (North–Holland, Amsterdam, 1985); (b) A. O. Langford, V. M. Bierbaum, and S. R. Leone, J. Chem. Phys. **83**, 3913 (1985).
[45]A. F. Wagner, J. Bowman, and L. B. Harding, J. Chem. Phys. **82**, 1866 (1985).
[46](a) Y. T. Lee, J. M. Bowman, A. F. Wagner, and G. C. Schatz, J. Chem. Phys. **76**, 3583 (1982); (b) J. M. Bowman, A. F. Wagner, S. P. Walch, and T. H. Dunning, Jr., *ibid.* **81**, 1739 (1984); (c) G. C. Schatz, A. F. Wagner, S. P. Walch, and J. M. Bowman, *ibid.* **74**, 4984 (1981).
[47]A. C. Luntz, J. Chem. Phys. **73**, 1143 (1980).
[48]J. F. Cordova, C. T. Rettner, and J. L. Kinsey, J. Chem. Phys. **75**, 2742 (1981).
[49](a) P. M. Aker, J. J. A. O'Brien, and J. J. Sloan, J. Chem. Phys. **84**, 745 (1986); (b) P. M. Aker, J. J. A. O'Brien, and J. J. Sloan, Chem. Phys. **104**, 421 (1986).
[50]S. Klee, K. H. Gehricke, and F. J. Comes, Chem. Phys. Lett. **118**, 530 (1985).
[51]M. S. Fitzcharles and G. C. Schnatz, J. Phys. Chem. **90**, 3634 (1986).